Copernicus Climate Change

# Integration of Climate Data in the SAVi Wastewater Model

## C3S_428h_IISD-EU: Sustainable Asset Valuation (SAVi): Demonstrating the Business Case for Climate-Resilient and Sustainable Infrastructure

Issued by: IISD-EU / Oshani Perera

Date: September 2020

Ref:

C3S_428h_IISD-EU_D428h.1.1 _202006_Integration of climate data in the SAVi model_v2

Official reference number service contract:

2019/C3S_428h_IISD-EU/SC1

# Contributors

**International Institute for Sustainable Development**
Bechauf, Ronja
Casier, Liesbeth
Lago, Sergio
Perera, Oshani
Perrette, Mahé
Uzsoki, David
Wuennenberg, Laurin

**KnowlEdge Srl**
Bassi, Andrea M.
Pallaske, Georg

## Table of Contents

# 1 About this Report

This report outlines the integration of authoritative Copernicus Climate Data from the Climate Data Store (CDS) into a Sustainable Asset Valuation (SAVi). It describes how several climate indicators obtained from the Copernicus CDS were integrated into the SAVi Wastewater model and how the analysis performed by SAVi has improved as a result. In light of this integration, IISD is able to generate sophisticated SAVi-derived analyses on the costs of climate-related risks and climate-related externalities.

The integration of Copernicus Climate Data into other SAVi models for energy, roads, irrigation, buildings, and nature-based infrastructure can be found here.

This document presents:
- A summary of the literature review on the climate impact on buildings, including the equations that link climate variables to the performance of buildings.
- How the above information was used to select relevant indicators from the Copernicus database.
- How outputs of the CDS datasets are integrated into the SAVi System Dynamics (SD) Wastewater model.
- How simulation results can be affected by the use of this new and improved set of indicators

This report is organized as follows.

**Literature review**

The literature review contains the following subsections for each of the climate variables discussed for wastewater treatment infrastructure:

- Subsection 1: An overview of climate impact on the asset (e.g., how precipitation affects wastewater treatment infrastructure).
- Subsection 2: A presentation of research results found in papers/reports that provide case studies on the range of impacts estimated or observed (e.g., across countries).
- Subsection 3: A description of the methodology found in the literature for the calculation of climate impacts on the infrastructure asset.
- Subsection 4: A selection of CDS datasets required by the equations.

**Integration of the Literature Review With the CDS Dataset**

This section summarizes information on what datasets are being used from the Copernicus database and what additional processing was applied before integrating these into the SAVi Wastewater model. We first review the equations to determine their usefulness for the SAVi Wastewater model. We then assess what data requirements for each of the equations are available in the Copernicus database and create indicators for climate variables that are relevant for the equations selected. Finally, in certain cases we create indicators in the CDS Toolbox for first-order impacts on wastewater treatment infrastructure. Second- and third-order impacts will be estimated with SAVi, making use of additional equations included in the SD model.

**Integration of Climate Indicators Into the SAVi Wastewater Model**

This section explains how the CDS indicators are used in the SAVi SD model for wastewater treatment infrastructure. It includes an identification of specific performance indicators for each asset impacted by climate indicators (e.g., efficiency and cost).

**Behavioural Impacts Resulting From the Integration of Climate Variables**

This section discusses how climate variables affect asset performance in the SD model, providing early insights as to how the results of the SAVi analysis may change when equipping the model with more and better refined climate indicators (e.g., with the cost of wastewater treatment infrastructure being higher due to increased maintenance, the economic viability of the infrastructure asset, expressed as the Internal Rate of Return [IRR], will be lower than expected).

**Simulation Results**

The final section of this paper presents equations used and quantitative results emerging from the inclusion of climate indicators in the SAVi Wastewater model under various climate scenarios. This is the end product of the enhanced SAVi model, which is used to inform policy and investment decisions for infrastructure. Table 1 provides an overview of climate drivers, impacts and relevant SAVi output indicators for wastewater treatment infrastructure.

The CDS datasets are accessed via the CDS application programming interface (API), and additional processing and packaging for use in SAVi is done offline. Technical information about the offline code is found in Annex I. We also selected a subset of the most-used indicators and created an app in the CDS Toolbox with interactive visualization for demonstration purposes.

Table 1. Overview of variables and impacts implemented into the SAVi Wastewater model

| **SAVi module** | **Implemented impact** | **Main climate drivers** | **Affected output indicators** |
|---|---|---|---|
| **Wastewater** | Urban stormwater runoff | • Precipitation | • Wastewater energy use<br>• Energy-related cost<br>• Nutrient removal<br>• Environmental cost of nutrients<br>• Social cost of carbon |
| | Urban flood indicator | • Precipitation | • Wastewater energy use<br>• Energy-related cost |

| SAVi module | Implemented impact | Main climate drivers | Affected output indicators |
|---|---|---|---|
| | | | • Nutrient removal<br>• Environmental cost of nutrients<br>• Social cost of carbon |
| | Effect of temperature on wetland phosphorus removal efficiency | • Temperature | • Phosphorus removal in wetlands<br>• Water quality<br>• Phosphorus-related mitigation costs<br>• Eutrophication<br>• Tourism revenues<br>• Fishery revenues |

# 2 Wastewater treatment infrastructure

## 2.1 Literature review

### 2.1.1 Capacity utilization

The amount of water treated by a Wastewater Treatment Facility (WWTF) is primarily a function of capacity and technical efficiency. On the other hand, there are several climate-related factor that affect both the extent to which the WWTF can be used, and how effectively. Impacts include among others high rainfall, which can lead to overflow (and hence reduces effectiveness); increased temperature, resulting in the growth of algae (and hence reduces effectiveness); as well as climate-induced power cuts, which reduce the operation time of the WWTF (and hence reduces effectiveness).

#### 2.1.1.1 Precipitation

- **Climate impact**

Precipitation impacts wastewater treatment plants in various ways: it can lead to overflow, due to runoff, affecting the efficiency of water treatment and the cost of operations; excessive water flow can lead to the shutdown of the wastewater treatment facility (WWTF).

#### 2.1.1.2 Runoff

- **Methodology**

Equation used in many articles to calculate runoff (Poullain, 2012):

$$Q = C * i * A$$

Q = peak rate of runoff in cubic feet per second (cfs)
C = runoff coefficient, a dimensionless unit
i = average intensity of rainfall in inches per hour (in/hr)
A = the watershed area in acres (ac).

A typical range for runoff coefficients is provided by Bengtson (2020) (see Figure 37):

Figure 1 Runoff coefficients

| Type of Area | Typical Range for Runoff Coefficient |
|---|---|
| Concrete Pavement | 0.70-0.95 |
| Park or Cemetary | 0.10-0.25 |
| Downtown Business | 0.70-0.95 |
| Single Family Residential Area | 0.30-0.50 |

**Considerations for integration in the CDS toolbox**

- ERA5-Land monthly averaged data from 1981 to present
- CMIP5 monthly data on single levels

#### 2.1.1.3 Overflow

- **Methodology**

Precipitation can cause overflow of wastewater, given that sewage systems are created to manage wastewater rather than total runoff. Literature shows that several categories of damages to road infrastructures can be related to distinct degrees of extreme precipitation. Specifically, the EWENT project (Extreme Weather impacts on European Networks of Transport) indicates the following (Nemry & Demirel, 2012):

- 50 mm/24h: flooded roads, reduced pavement fraction;
- 100 mm/24h: the sewer system fills up; water rises up the streets from drains. Rainwater fills the underpasses and lower laying streets. Drain well covers may become detached and cause danger to street traffic. Reduced visibility, flooded underpasses
- 150 mm/24h: road structures may collapse. Bridges may be flooded. Vehicle motors damaged and vehicle can be flooded. Roads might be covered by water or transported debris.

As a result, a non-linear function generating an index of severity of the rainfall events, based on precipitation per day, could be created (y=f(x)).

Severity of rainfall = [(0, 0), (50, 1), (100, 2), (150, 3)] (precipitation per day).

#### 2.1.1.4 Temperature

- **Climate impact**

Changes in temperatures for wastewater treatment change the efficiency of removal of pollutants. Higher water temperature allow the creation of algae and other parasites that reduce the efficiency of treatment and increase the amount of time required to treat the same quantity of water. At the same time, higher temperature leads to the reduction of the concentration of other pollutants, increasing efficiency. Impacts vary depending on the pollutant to be removed.

Higher temperature have a second possible impact, on water quantity. If higher temperatures reduce water availability, the plant will have to stop operations.

- **Summary of results**

For precision: SS= Suspended solids; COD=Chemical Oxygen Demand; $PO_4^{3-}$ = Phosphate; $NO^-_3$ = Nitrate; $NH^+_4$ = Ammonium.
Removal efficiency of nutrients varies in wastewater treatment with refuse cement or concrete.
The first one for [SS; COD; $PO_4^{3-}$; $NO^-_3$; $NH^+_4$] removal efficiency from 20˚C to 40˚C has an increase for a median particle size of 0.43 of [29%; 51%; 1%; -33%; 20%] respectively. For the second one, with same parameters, removal efficiency change is [11%; 14%; -34%; 5%; 15%].
Specifically for nitrogen, from a base case of influent sewage temperature of 7-10 ˚C and removal efficiency of 75-80%, a change of -1.5 to +5˚C impacts nitrogen removal efficiency by -6% per 1˚C in influent sewage temperature.

- **Results**

Ahsan et al. (2005) estimated the removal efficiency of a wastewater plant for different pollutants when there are increasing temperatures (see Figure 38).

Figure 2 Pollutant removal efficiency and temperature

**Table 1** Effect of temperature on the wastewater treatment with refuse cement and refuse concrete

| Treatment medium | Pollutant | Temperature (°C) | Removal efficiency (%) Particle diameter (mm) | | | |
|---|---|---|---|---|---|---|
| | | | 0.30 | 0.35 | 0.43 | 0.60 |
| Refuse cement | SS | 20 | 95 | 82 | 71 | 73 |
| | | 40 | 97 | 92 | 100 | 94 |
| | COD | 20 | 40 | 25 | 24 | 29 |
| | | 40 | 74 | 77 | 75 | 84 |
| | $PO_4^{3-}$ | 20 | 92 | 90 | 89 | 92 |
| | | 40 | 90 | 90 | 90 | 89 |
| | $NO_3^-$ | 20 | 23 | 25 | 33 | 20 |
| | | 40 | 0 | 0 | 0 | 0 |
| | $NH_4^+$ | 20 | 34 | 10 | 10 | 34 |
| | | 40 | 35 | 29 | 30 | 36 |
| Refuse concrete | SS | 20 | 92 | 77 | 87 | 71 |
| | | 40 | 98 | 96 | 98 | 93 |
| | COD | 20 | 53 | 47 | 46 | 35 |
| | | 40 | 65 | 57 | 60 | 62 |
| | $PO_4^{3-}$ | 20 | 90 | 47 | 70 | 50 |
| | | 40 | 54 | 30 | 36 | 20 |
| | $NO_3^-$ | 20 | 32 | 26 | 28 | 28 |
| | | 40 | 43 | 40 | 33 | 38 |
| | $NH_4^+$ | 20 | 58 | 58 | 12 | 24 |
| | | 40 | 24 | 30 | 27 | 13 |

$n = 3$

In a case study in Norway, Plósz et al. (2009) reported that at low daily air mean temperatures, heat transported by the influent sewage into the WWTP can be characterized with liquid temperatures between 7 and 10˚C, and with high biological nitrogen removal efficiencies (75–80%). Moreover, during temporary increases of air temperature (-1.5 to + 5C), nitrogen removal efficiency decreases by 6% per 1˚C degree decrease in the influent sewage temperature (see Figure 39).

Figure 3 Nitrogen removal efficiency and sewage temperature

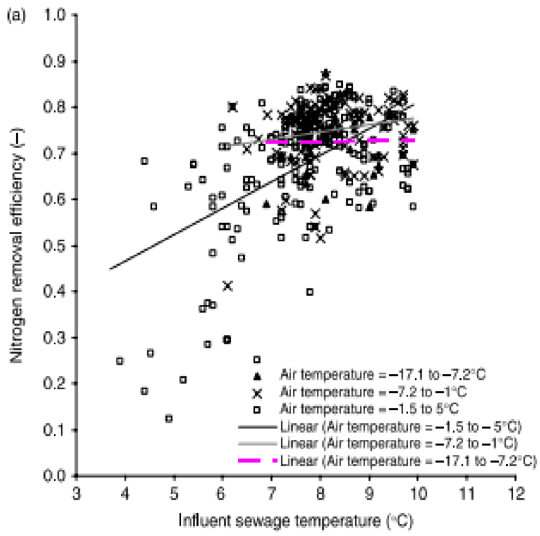


In China, three SWIS (Soil wastewater infiltration system) efficiency has been studied under different temperatures by Yuan et al. (2013). All the SWIS were operated at a hydraulic loading of 26 cm/day, COD of 233 mg/L for 10 weeks at the influent wastewater temperature of 7 ◦C, 13 ◦C, 18 ◦C, 25 ◦C and 33 ◦C, respectively.

- COD decreased sharply when the temperature was less than 13◦C, meanwhile the removal efficiency of COD was between 83.3% and 95.0% in the treatment of the soil column. While the operation temperature was increasing until to 33◦C, the effluent COD concentration decreased gradually to a very low level, and the COD removal efficiency could reach as high as 98.3%.
- NH3-N: At the temperature of 7 ◦C, the average removal efficiency was below 85%, and the NH3- N concentration of effluent from the experimental soil column was about 4.0 mg/L. When temperature was about 13 ◦C, the NH3-N concentration of effluent decreased from 4.0 mg/L to 1.0 mg/L and the average removal rate could reach as high as 97.1% when the SWIS operation temperature was higher than 13 ◦C.
- TN: When the operation temperature of the SWIS was lower than 25 ◦C, the removal efficiency of TN was between 60.0% and 75.0%. Furthermore, the highest removal efficiency of TN could reach 85.0% when the SWIS was operated at 33 °C.
- TP: No effect

- **Methodology**

Method 1 (Singh & Tiwari, Climate Change, Water and Wastewater Treatment: Interrelationship and Consequences, 2019)

Rate of biological reaction (sedimentation): k = k20ϴ T-20

K is reaction rate constant at temperature, T
k20 = reaction rate constant at 20˚C
ϴ = temperature coefficient
T = temperature of biological reaction.

**Considerations for integration in the CDS toolbox**

ERA5-Land monthly averaged data from 1981 to present
CMIP5 monthly data on single levels

Method 2 (Zsirai, Buzatu, Maffettone, & Judd, 2012)

Impact of temperature on viscosity. The change in the viscosity of water (in mPa s) with temperature within the limits of 5 and 35°C can, within an R2 value of 0.9995, be represented by the following quadratic equation:

$$\mu_w = 5.829 \times 10^{-5} T^2 - 4.868 \times 10^{-2}\, T + 0.00174$$

Another article, from Ronda and van der Graaf (2000) is cited with another regression:

$$\mu = 497\,(T + 42.5)^{-1.5}$$

**Considerations for integration in the CDS toolbox**

ERA5-Land monthly averaged data from 1981 to present
CMIP5 monthly data on single levels

## 2.2 Integration of literature review with the CDS datasets

See section 1.2 for explanations how we selected the indicators to implement in the CDS Toolbox. Similarly to 1.2, each variable is available in two versions, ERA5 reanalysis (single level, monthly) for past data (2000-2019) and CMIP5 (single level, monthly) for future data (2006-2100).

The work performed with the CDS Toolbox is available at these links:

- Source code: https://cds.climate.copernicus.eu/toolbox-editor/27053/indicator-download
- App: https://cds.climate.copernicus.eu/apps/27053/indicator-download

Datasets:

- ERA5 monthly data on single level: 2000 to 2019
- CMIP5 monthly data on single level: 2006 to 2100

Indicators created:

- **Precipitation**:
  - Units: mm per month
  - Frequency: monthly
  - ERA5 variable: “Mean total precipitation rate”
  - CMIP5 variable: “Mean precipitation flux“
  - Note: original units in mm/s
- **Runoff**
  - Units: mm per month
  - Frequency: monthly
  - ERA5 variable: “Mean runoff rate”
  - CMIP5 variable: “Runoff“
  - Note: original units in mm/s
- **Air temperature**
  - Units: degrees Celsius
  - Frequency: monthly
  - ERA5 variable: “2 m temperature”
  - CMIP5 variable: “2 m temperature“
  - Note: original units in Kelvin

## 2.3 Integration of climate indicators into the SAVi wastewater model

CDS climate indicators related to wastewater include impacts on wastewater volumes in the sewage system, wastewater treatment efficiency-and capacity depreciation. The CLD of the SAVi Wastewater model is presented in Figure 40. Climate indicators obtained from the CDS database are highlighted in pink.

Figure 4 Causal Loop Diagram for the wastewater sector - CDS variables included

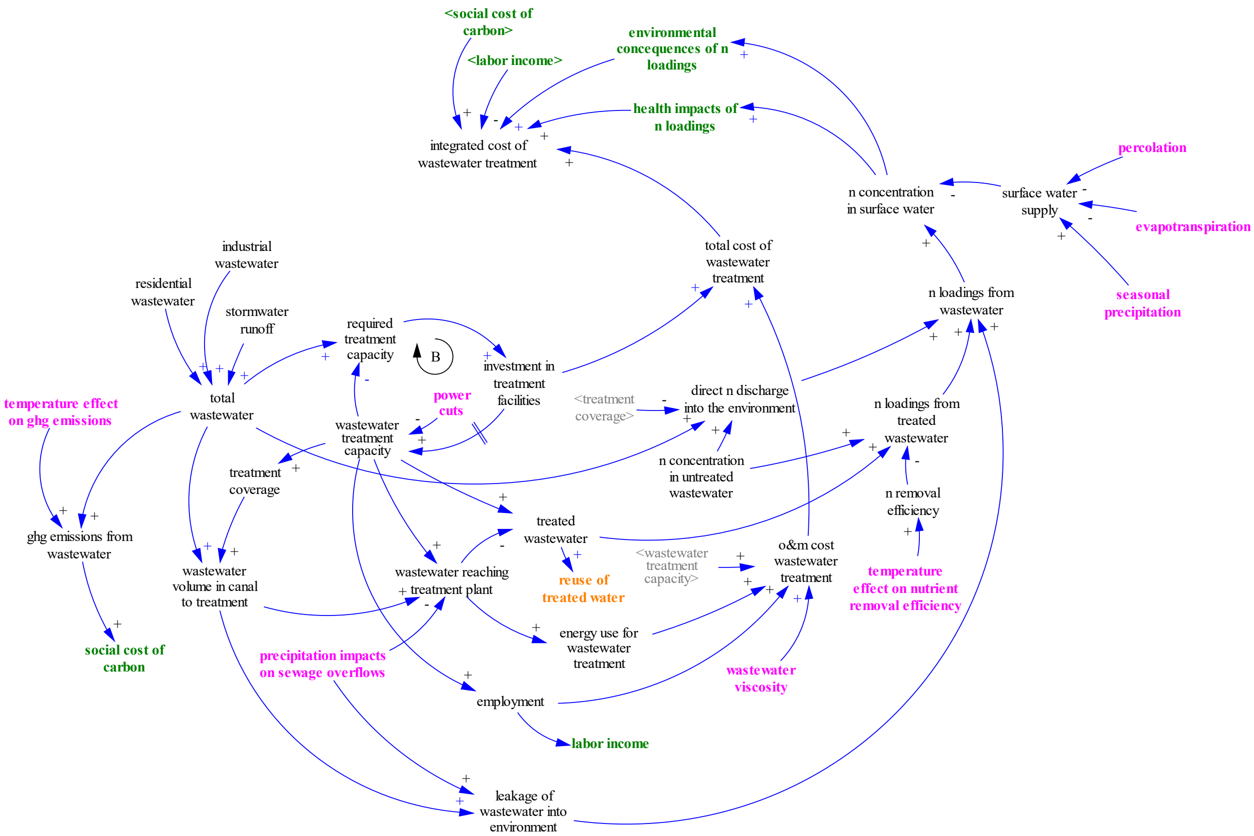


Climate change impacts on wastewater volumes refers to (i) sewage overflows due to excessive water flow during precipitation events, (ii) a reduction in total sewage flow volume due to decreases in water volume, while pollution loads remain the same, and (iii) increased viscosity of water. During sewage overflows, vast amounts of water enter the sewage system within a short period of time. The stormwater mixes with the sewage, and once the total waste- and stormwater volume exceeds sewage capacity, wastewater is flushed into the streets and leaks into the environment. On the opposite hand, low precipitation may reduce the flow of water and the amount that is effectively treated. In addition, low precipitation and higher temperatures, combined with unchanged pollution creation, increase the viscosity of wastewater. This reduces flow speed in the sewage system and causes increased system corrosion in sewers and wastewater treatment plants, also resulting in higher operation and maintenance costs.

The wastewater treatment efficiency indicator developed from the CDS toolbox refers to impacts on nutrient removal efficiency in treatment plants. Warmer temperatures benefit nutrient removal efficiencies and are a requirement for the use of certain wastewater treatment technologies.

## 2.4 Behavioral impacts resulting from the integration of climate variables

The sewage overflow indicator obtained from the CDS toolbox forecasts seasonal changes in stormwater loads and the occurrence of sewage overflows. This allows to improve the estimation of leakage in the SAVi model, and better represent the concentration of pollutants in waterbodies, related environmental impacts and costs.

Furthermore, wastewater treatment efficiency is reduced during peak flow events that exceed the capacity of WWTF. This is because of the lower amount of water treated and the reduced concentration of pollutants in the wastewater treated.

The CDS Toolbox will also support the estimation of wastewater treatment efficiency using seasonal data. This is important due to the higher impact of wastewater and related pollutants during months with warm climate and months with low precipitation. Viscosity affects maintenance costs, nutrient removal impacts energy use for treatment and hence also affects operation costs of WWTFs. In addition to operation costs, removal efficiency determines the total capacity requirement of a wastewater system.

Specifically on viscosity, the use of the CDS Toolbox indicator on sewage viscosity is used to forecast accelerated depreciation of wastewater treatment infrastructure (sewers and treatment plants). An increase in viscosity leads to increased settlement of sludge in sewers, increasing maintenance cost for dredging, and the accelerated depreciation leads to shorter asset lifetime and increased replacement capital cost.

## 2.5 Simulation results

The dynamics of wastewater treatment and its efficiency depend on wastewater loads remaining within the capacity of sewers and sewage treatment plants. The following additions were implemented into the SAVi Wastewater treatment model: (1) urban flood indicator, and (2) stormwater runoff per hectare. While the flood indicator allows to forecast the amount of months with extreme stormwater loads, the actual stormwater runoff per hectare provides information about the forecasted total loads that occur during one month. The total area considered for the results presented below is 10 hectares.

### 2.5.1 Impact of heavy precipitation on urban flooding

Heavy precipitation events cause urban flooding and contribute to sewage overflows. Sewage overflow is caused by vast storm- and wastewater loads into sewers that exceed their capacity.

The urban flood indicator is based on below mentioned precipitation thresholds provided by Nemry and Demirel (2012).

| Precipitation (mm/hr) | Expected impact |
|---|---|
| 50mm-100mm | flooded roads |
| 100mm-150mm | sewer overflows and potential impacts on traffic |
| >150mm | severe flooding, roads may collapse and bridges flooded; vehicle damages will occur |

Table 2: Precipitation thresholds and their impact on urban flooding (Nemry & Demirel, 2012)

The SAVi model is operationalized using monthly precipitation data, therefore relative monthly precipitation is used to determine the potential flooding that may occur. The thresholds for relative precipitation used for this illustration are listed in Table 14.

| Relative precipitation | Projected impact |
|---|---|
| 0-2 | No impacts |
| 2-3 | Flooded roads |
| 3-4 | sewer overflows and potential impacts on traffic |
| >5 | severe flooding, roads may collapse and bridges flooded; vehicle damages will occur |

Table 3: Thresholds for relative precipitation used for the operationalization of urban flooding in the SAVi wastewater model

The equation used for the calculation of the urban flood indicator is described below.

*Urban flood indicator = IF THEN ELSE ( Relative precipitation > Threshold for urban flooding, Relative precipitation / Threshold for urban flooding, 1)*

The urban flood indicator is used as a multiplier in the model, indicating that a value of 1 will result in no impact of flooding, while any month during which precipitation exceeds the threshold value will see an increased risks of floods. The resulting flood indicator values for Johannesburg are presented in Figure 41 for the period 1979 to 2100.

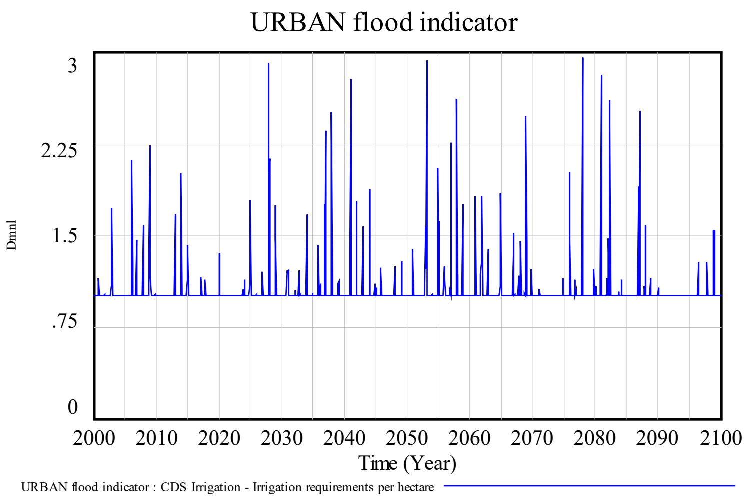


Figure 5: Flood indicator for Johannesburg IPSL RCP8.5 scenario

The effect of urban flooding on sewage overflows is implemented using the flood indicator and an assumption on the percentage that flows out with each 1 point increase of the flood indicator. The percentage assumed for this simulation is 10%, indicating that if the flood indicator value increases from 3 to 4, and additional 10% will flow out of sewers during that month. An IF THEN ELSE function is used to ensure that there is no outflow if the indicator has a value of 1 (default value in case of no impacts). The amount of water that flows out of the sewers is presented in Figure 42.

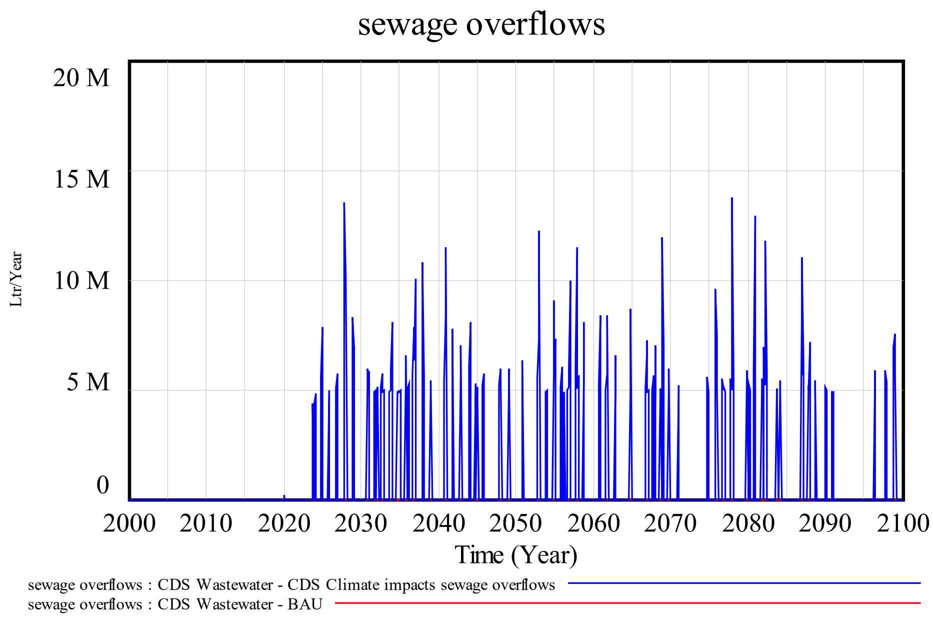


Figure 6: Projected sewage overflows Johannesburg

The simulation results indicate higher energy use in the sewage overflow scenario, resulting in higher energy costs and energy related emissions. Between 2020 and 2080, the cumulative energy use for wastewater treatment in the CDS climate impact scenario is projected to be 2.25% higher, which is equivalent to 679 MWh over 80 years, or approximately 8.5 MWh per year on average. The model indicates that, despite the reduction in the share of wastewater treated induced by the sewage overflow formulation, the total amount of nitrogen removed is 2.25% higher[1].

Energy costs are assumed at 20 cents per kWh and emissions are estimated using total energy use for N removal and an average grid emission factor of 0.7 tons per MWh. Emissions are valued using the Social Cost of Carbon, based on Nordhaus (2017), using 31 USD per ton of CO2e without escalation. In addition, sewage overflows cause wastewater to leak into the environment, which can have detrimental consequences for ecosystems and land productivity (UNEP, 2015)[2]. A value of USD 4.9 per kg N is applied to estimate the additional cost of N leaking into the environment and the avoided environmental damages through wastewater treatment. Table 15 provides an overview of the economic performance for selected indicators of the wastewater treatment sector.

| Indicator | No impacts | (1) Sewage overflow | (1) vs no impact |
|---|---|---|---|

[1] The difference in energy use is mainly driven by two factors: (1) new precipitation inputs obtained from the CDS database (pushing energy consumption higher relative to the no impact scenario), and (2) the impact of sewage overflows (reducing energy consumption).

[2] A value of USD 4.9 per kg N (EUR 4.6) released into the environment is assumed for the estimation of N related environmental damages and the avoided environmental cost of disposing N into the environment. The values indicated in UNEP (2015) range from EUR 4.6 per kg N released into the open sea to EUR 65.2 per kg N released into wetlands.

| | | | |
|---|---|---|---|
| Energy cost for wastewater treatment | 6,036,634 | 6,172,436 | 135,803 |
| Cost of n leaching into the environment | 0 | 204,343 | 204,343 |
| Social cost of carbon from wastewater treatment | 654,975 | 669,709 | 14,735 |
| **Total costs and externalities** | **6,691,608** | **7,046,488** | **354,880** |
| Avoided environmental damages through wastewater treatment | 5,915,901 | 6,048,988 | 133,087 |
| **Net societal cost of wastewater treatment** | **775,707** | **997,500** | **221,793** |

Table 4: Monetized impacts of sewage overflows

### 2.5.2 Climate impacts on urban runoff

Information about urban runoff is important for urban infrastructure planners to ensure capacity adequacy of sewage system capacity and potential mitigation requirements. The stormwater runoff per hectare in urban areas is calculated using the following equation:

*Runoff quantity = Average intensity of monthly rainfall * runoff coefficient * conversion from mm to liters per hectare*

Figure 43 presents the simulation results for stormwater runoff in urban areas in the no impact and the CDS climate impact scenario. The results show a significant difference in variability and magnitude of stormwater runoff in the CDS climate impact scenario.

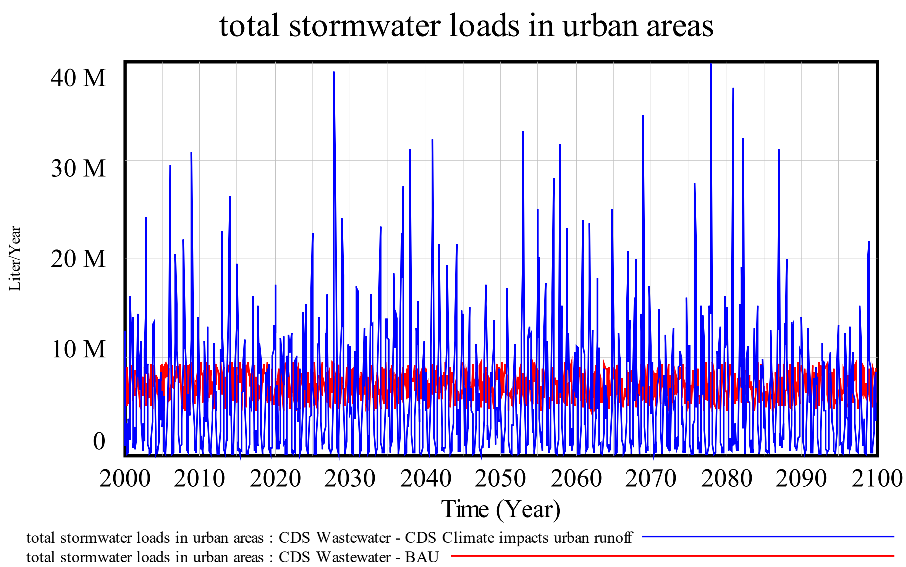


Figure 7: Urban stormwater runoff per hectare

The results indicate a cumulative total stormwater load of 6.7 billion liters and 5.83 billion liters in the no climate and climate impact scenario respectively between 2020 and 2100. The change in simulation results us equivalent to a reduction of 13% in cumulative stormwater loads in the CDS climate impact scenario compared to the no impact scenario. The above indicates that the updated formulation allows for introducing extreme precipitation events into the analysis, while estimating stormwater loads more accurately. For example, while the maximum monthly stormwater load projected in this example is 37.8 million liters in the CDS climate impact scenario, which is more than four times the amount of the 9.5 million liters indicated in the no impact scenario.

The increased stormwater loads increase the total energy use of the wastewater treatment system. Compared to the no impact scenario, total energy use is projected to be 5.4% higher, which is equivalent to 20.33 MWh per year or approximately 1,627 MWh over 80 years. Consequently, the energy cost and social cost of carbon are higher in the CDS impact scenario compared to the no impact scenario. This CDS impact scenario assumes that the urban stormwater runoff does not cause sewage overflows, hence no additional cost of N reaching the environment incur.

| Indicator | No impacts | (2) Urban flooding | (2) vs no impact |
|---|---|---|---|
| Energy cost for wastewater treatment | 6,036,634 | 6,362,023 | 325,390 |
| Cost of n leaching into the environment | 0 | 0 | 0 |
| Social cost of carbon from wastewater treatment | 654,975 | 690,280 | 35,305 |
| **Total costs and externalities** | **6,691,608** | **7,052,303** | **360,695** |
| Avoided environmental damages through wastewater treatment | 5,915,901 | 6,234,783 | 318,882 |
| **Net societal cost of wastewater treatment** | **-775,707** | **-817,520** | **-41,813** |

Table 5: Monetized impacts of urban stormwater runoff

# 3 Bibliography

Acclimatise. (2009). *Building Business Resilience to Inevitable Climate Change. Carbon Disclosure Project Report. Global Electric Utilities.* Oxford.

Adeh, E. H., Good, S. P., Calaf, M., & Higgins, C. W. (2019). Solar PV Power Potential is Greatest Over Croplands. *Scientific reports, vol(9), no(1)*, pp. 1-6.

Ahsan, S., Rahman, M. A., Kaneco, S., Katsumata, H., Suzuki, T., & Ohta, K. (2005). Effect of temperature on wastewater treatment with natural and waste materials. *Clean Technologies and Environmental Policy, 7(3)*, 198-202.

Akbari, H. (2005). *Energy saving potentials and air quality benefits of urban heat island mitigation.* Récupéré sur OSTI.org: https://www.osti.gov/biblio/860475/

Akbari, H., Davis, S., Dorsano, S., Huang, J., & Winnett, S. (1992). *Cooling our communities: A guidebook on tree planting and light-colored surfacing.* Washington, DC (United States): Lawrence Berkeley Lab.; Environmental Protection Agency.

Alam, T., Mahmoud, A., Jones, K. D., Bezares-Cruz, J. C., & Guerrero, J. (2019). A Comparison of Three Types of Permeable Pavements for Urban Runoff Mitigation in the Semi-Arid South Texas, USA. *MDPI - Water, 11(10)*.

Allen, R. G., Pereira, L. S., Raes, D., & Smith, M. (2006). *FAO Irrigation and Drainage Paper - Crop Evapotranspiration.* FAO.

Allos, M. (2016, Juin). *Potential Damage Caused by Direct Lightning Strikes*. Récupéré sur Sollatek: https://www.sollatek.com/potential-damage-caused-direct-lightning-strikes/

American Society of Landscape Architects. (2003). *Chicago City Hall Green Roof*. Récupéré sur asla.org: http://www.asla.org/meetings/awards/awds02/chicagocityhall.html

Asian Development Bank. (2012). *Adaptation to Climate Change - The Case of a Combined Cycle Power Plant.* Philippines.

Attia, S. I. (2015). The influence of condenser cooling water temperature on the thermal efficiency of a nuclear power plant. *Annals of Nuclear Energy*, 371-378.

Bartos, M., Chester, M., Johnson, N., Gorman, B., Eisenberg, D., Linkov, I., & Bates, M. (2016). Impacts of rising air temperatures on electric transmission ampacity and peak electricity load in the United States. *Environmental Research Letters, 11(11), 1*.

Basha, M., Shaahid, S. M., & Al-Hadhrami, L. (2011). Impact of fuels on performance and efficiency of gas turbine power plants. *2nd International Conference on Advances in Energy Engineering*, (pp. 558-565). Bangkok.

Bassi, A. M., Pallaske, G., Wuennenberg, L., Graces, L., & Silber, L. (2019, March). *Sustainable Asset Valuation Tool: Natural Infrastructure.* Récupéré sur International Institute for Sustainable Development : https://www.iisd.org/sites/default/files/publications/sustainable-asset-valuation-tool-natural-infrastructure.pdf

Bengtson, H. (2020). *The Rational Method for Estimation of Design Surface Runoff Rate for Storm Water Control*. Récupéré sur brighthubengineering.com: https://www.brighthubengineering.com/hydraulics-civil-engineering/60842-the-rational-method-for-calculation-of-peak-storm-water-runoff-rate/

Bergel-Hayat, R., Debbarh, M., Antoniou, C., & Yannis, G. (2013). Explaining the road accident risk: weather effects. *Accident Analysis & Prevention, 60*, 456-465.

Berghage, R. D., Beattie, D., Jarrett, A. R., Thuring, C., Razaei, F., & O'Connor, T. P. (2009). *Green Roofs For Stormwater Runoff Control.* Cincinnati: EPA.

Bhatt, S., & Rajkumar, N. (2015). Effect of moisture in coal on station heat rate and fuel cost for Indian thermal power plants. *Power Research, 11(4)*, 773-786.

Bhattacharya, C., & Sengupta, B. (2016). Effect of ambient air temperature on the performance of regenerative air preheater of pulverised coal fired boilers. *Int. J. Energy Technology and Policy, Vol. 12, No. 2*, pp. 136–153.

Biswas, B. (2014). Construction and Evaluation of Rainwater Harvesting System for Domestic Use in a Remote and Rural Area of Khulna, Bangladesh. *International Scholarly Research Notices*. doi:https://doi.org/10.1155/2014/751952

Brouwer, C., & Heibloem, M. (1986). Irrigation Water Management and Irrigation Water Needs. *FAO - Training manual, 3.*

Brouwer, C., Prins, K., & Heibloem, M. (1989). *Irrigation water management: irrigation scheduling.* Récupéré sur Fao.org: http://www.fao.org/3/T7202E/t7202e00.htm#Contents

Büyükalaca, O., Bulut, H., & Yılmaz, T. (2001). Analysis of variable-base heating and cooling degree-days for Turkey. *Applied Energy, 69(4)*, pp. 269-283.

Carnegie Mellon University (CMU). (s.d.). *Integrated Environmental Control Model.* Récupéré sur Department of Engineering & Public Policy (EPP): https://www.cmu.edu/epp/iecm/

Chinowsky, P. S., Price, J. C., & Neumann, J. E. (2013). Assessment of climate change adaptation costs for the US road network. *Global Environmental Change, 23(4)*, 764-773.

Chinowsky, P., Hayles, C., Schweikert, A., Strzepek, N., Strzepek, K., & Schlosser, A. (2011). Climate change: comparative impact on developing and developed countries. *The Engineering Project Organization Journal*, pp. 67-80.

Choi, T., Keith, L., Hocking, E., Friedman, K., & Matheu, E. (2011). *Dams and energy sectors interdependency study.*

City of Chicago Department of Environment. (2006). *Green roof test plot project: annual project summary report.* Chicago.

Colman, J. (2013, Avril 26). The effect of ambient air and water temperature on power plant efficiency. *Master Thesis*. Duke University Libraries.

Cronshey, R., McCuen, R. H., Miller, N., Rawls, W., Robbins, S., & Woodward, D. (1986, June). *Urban Hydrology for Small Watersheds.* Récupéré sur USDA-United States Department of Agriculture: https://www.nrcs.usda.gov/Internet/FSE_DOCUMENTS/stelprdb1044171.pdf

Das, T. K., Saharawat, Y. S., Bhattacharyya, R., Sudhishri, S., Bandyopadhyay, K. K., Sharma, A. R., & Jat, M. L. (2018). Conservation agriculture effects on crop and water productivity, profitability and soil organic carbon accumulation under a maize-wheat cropping system in the North-western Indo-Gangetic Plains. *Field Crops Research, 215*, pp. 222-231.

Davies, Z. G., Edmondson, J. L., Heinemeyer, A., Leake, J. R., & Gaston, K. J. (2011). Mapping an urban ecosystem service: quantifying above-ground carbon storage at a city-wide scale. *Journal of applied ecology, 48(5)*, pp. 1125-1134.

Davy, R., Gnatiuk, N., Pettersson, L., & Bobylev, L. (2018). Climate change impacts on wind energy potential in the European domain with a focus on the Black Sea. *Renewable and sustainable energy reviews*, pp. 1652-1659.

De Oliveira, V., De Mello, C., Viola, M., & Srinivasan, R. (2017). Assessment of climate change impacts on the streamflow and hydropower potential in the headwater region of the Grande river basin, Southeastern Brazil. *International Journal of Climatology 37[15]*, pp. 5005-5023.

De Rosa, M., Bianco, V., Scarpa, F., & Tagliafico, L. A. (2014). Heating and cooling building energy demand evaluation; a simplified model and a modified degree days approach. *Applied Energy, 128*, 217-229.

De Sa, A., & Al Zubaidy, S. (2011). Gas turbine performance at varying ambient temperature. *Applied Thermal Engineering, 31(14-15)*, 2735-2739.

Demuzere, M., Orru, K., Heidrich, O., Olazabal, E., Geneletti, D., Orru, H., . . . Faehnle, M. (2014). Mitigating and adapting to climate change: Multi-functional and multi-scale assessment of green urban infrastructure. *Journal of environmental management, 146*, pp. 107-115.

Dhakal, S., & Hanaki, K. (2002). Improvement of urban thermal environment by managing heat discharge sources and surface modification in Tokyo. *Energy and buildings, 34(1)*, pp. 13-23.

Diaz, C. A., Osmond, P., & King, S. (2015). Precipitation and buildings: estimation of the natural potential of locations to sustain indirect evaporative cooling strategies through hot seasons. *Living and Learning: Research for a Better Built Environment: 49th International Conference of the Architectural Science Association*, (pp. 45-54). Melbourne.

Djaman, K., O'Neill, M., Owen, C. K., Smeal, D., Koudahe, K., West, M., & Irmak, S. (2018). Crop evapotranspiration, irrigation water requirement and water productivity of maize from meteorological data under semiarid climate. *MDPI - Water 2018, 10(4), 405*.

Doorenbos, J., & Kassam, A. (1979). *Yield response to Water Irrigation and Drainage.* Roma: Food and Agricultural Organization; Paper No 33.

Drax. (2017, August 29). *Technology - What hot weather means for electricity*. Récupéré sur Drax.com: https://www.drax.com/technology/hot-weather-means-electricity/

Du, L., Trinh, X., Chen, Q., Wang, C., Wang, H., Xia, X., . . . Wu, Z. (2018). Enhancement of microbial nitrogen removal pathway by vegetation in Integrated Vertical-Flow Constructed Wetlands (IVCWs) for treating reclaimed water. *Bioresource technology, 2*.

Dunn, A. D. (2007). *Green light for green infrastructure.* Récupéré sur Digitalcommons.pace.edu: https://digitalcommons.pace.edu/lawfaculty/494

Durmayaz, A., & Sogut, O. S. (2006). Influence of cooling water temperature on the efficiency of a pressurized-water reactor nuclear-power plant. *International Journal of Energy Research, 30(10)*, pp. 799-810.

East Coast Lightning Equipment INC. (s.d.). *Lightning protection installation cost study* . Récupéré sur East Coast Lightning Equipment INC: https://ecle.biz/coststudy/

Eliasson, J., & Ludvigsson, G. (2000). Load factor of hydropower plants and its importance in planning and design. *11th International Seminar on Hydro Power Plants.* Vienna.

El-Refaie, G. (2010). Temperature impact on operation and performance of Lake. *Ain Shams Engineering Journal 1*, 1-9.

El-Shobokshy, M. S., & Hussein, F. M. (1993). Degradation of photovoltaic cell performance due to dust deposition on to its surface. *Renewable Energy, 3(6-7)*, pp. 585-590.

Engineering ToolBox. (2009). *Pumping Water - Energy Cost Calculator*. Récupéré sur engineeringtoolbox.com: https://www.engineeringtoolbox.com/water-pumping-costs-d_1527.html

Engineering ToolBox. (s.d.). *Hydropower*. Récupéré sur Engineering ToolBox: https://www.engineeringtoolbox.com/hydropower-d_1359.html

EPA. (2014). *The Economic Benefits of Green Infrastructure - A Case Study of Lancaster, PA.*

Eurostat. (2019). *Energy statistics - cooling and heating degree days (nrg_chdd)*. Récupéré sur Eurostat, the Statistical Office of the European Union: https://ec.europa.eu/eurostat/cache/metadata/en/nrg_chdd_esms.htm

Eurostat, the Statistical Office of the European Union. (2019). *Energy statistics - cooling and heating degree days (nrg_chdd)*. Récupéré sur Europa.eu: https://ec.europa.eu/eurostat/cache/metadata/en/nrg_chdd_esms.htm

Evans, D. V., & Antonio, F. D. (1986). Hydrodynamics of Ocean Wave-Energy Utilization: IUTAM Symposium Lisbon/Portugal 1985. *Springer Science & Business Media*, pp. 133-156.

Farkas, Z. (2011). *Considering air density in wind power production.* Budapest.

Fisher, J. C., Bartolino, J. R., Wylie, A. H., Sukow, J., & McVay, M. (2016). *Groundwater-flow model for the Wood River Valley aquifer system, south-central Idaho.* US Geological Survey.

Flowers, M. E., Smith, M. K., Parsekian, A. W., Boyuk, D. S., McGrath, J. K., & Yates, L. (2016). Climate impacts on the cost of solar energy. *Energy Policy, 94*, pp. 264-273.

Gajbhiye, S., Mishra, S. K., & Pandey, A. (2013). Effects of Seasonal/Monthly Variation on Runoff Curve Number for Selected Watersheds of Narmada Basin. *International Journal of Environmental Sciences, Volume 3, No 6*, pp. 2019-2030.

Garfí, M., Pedescoll, A., Bécares, E., Hijosa-Valsero, M., Sidrach-Cardona, R., & García, J. (2012). Effect of climatic conditions, season and wastewater quality on contaminant removal efficiency of two experimental constructed wetlands in different regions of Spain. *Science of the total environment, 437*, pp. 61-67.

Georgi, N. J., & Zafiriadis, K. (2006). The impact of park trees on microclimate in urban areas. *Urban Ecosystems, 9(3)*, pp. 195-209.

Ghamami, M., Fayazi Barjin, A., & Behbahani, S. (2016). Performance Optimization of a Gas Turbine Power Plant Based on Energy and Exergy Analysis. *Mechanics, Materials Science & Engineering Journal, 29*.

GIZ. (2016). *Solar Powered Irrigation Systems (SPIS) – Technology, Economy, Impacts.* Récupéré sur Gesellschaft für Internationale Zusammenarbeit (GIZ): https://energypedia.info/images/temp/2/23/20160630122544!phpeKHVUr.pdf

Gomes, J., Diwan, L., Bernardo, R., & Karlsson, B. (2014). Minimizing the Impact of Shading at Oblique Solar Angles in a Fully Enclosed Asymmetric Concentrating PVT Collector. *Energy Procedia (57)*, pp. 2176-2185.

Good, E., & Calaf, S. (2019). Solar PV Power Potential is Greatest Over Croplands. *SciRep (9, 11442)*.

Green, A. (2020). *The intersection of energy and machine learning*. Récupéré sur adgefficiency.com: https://adgefficiency.com/energy-basics-ambient-temperature-impact-on-gas-turbine-performance/

Haerter, J., Hagemann, S., Moseley, C., & Piani, C. (2011). Climate model bias correction and the role of timescales. *Hydrology and Earth System Sciences, 15*, pp. 1065-1073.

Handayani, K., Filatova, T., & Krozer, Y. (2019). The Vulnerability of the Power Sector to Climate Variability and Change: Evidence from Indonesia. *Energies, 12(19), 3640*.

Harrison, G. P., & Whittington, H. W. (2002). Vulnerability of hydropower projects to climate change. *IEE proceedings-generation, transmission and distribution, 149(3)*, pp. 249-255.

Harrison, G., & Wallace, A. (2005). Climate sensitivity of marine energy. *Renewable Energy, 30(12)*, pp. 1801-1817.

Henry, C. L., & Pratson, L. F. (2016). Effects of environmental temperature change on the efficiency of coal-and natural gas-fired power plants. *Environmental science & technology, 50(17)*, 9764-9772.

Hutyra, L. R., Yoon, B., & Alberti, M. (2011). Terrestrial carbon stocks across a gradient of urbanization: a study of the Seattle, WA region. *Global Change Biology, 17(2)*, pp. 783-797.

Ibrahim, S., Ibrahim, M., & Attia, S. (2014). The impact of climate changes on the thermal performance of a proposed pressurized water reactor: nuclear-power plant. *International Journal of Nuclear Energy*.

Jabboury, B. G., & Darwish, M. A. (1990). Performance of gas turbine co-generation power desalting plants under varying operating conditions in Kuwait. *Heat Recovery Systems and CHP, 10(3)*, 243-253.

Jackson, N., & Puccinelli, J. (2006). *Long-Term Pavement Performance (LTPP) data analysis support: National pooled fund study TPF-5 (013)-effects of multiple freeze cycles and deep frost penetration on pavement performance and cost (No. FHWA-HRT-06-121).*

Janssen, H., Carmeliet, J., & Hens, H. (2004). The influence of soil moisture transfer on building heat loss via the ground. *Building and Environment, 39(7)*, 825-836.

Jerez, S., Tobin, I., Vautard, R., Montávez, J. P., López-Romero, J. M., Thais, F., . . . Wild, M. (2015). The impact of climate change on photovoltaic power generation in Europe. *Nature Communications, 6(1)*, pp. 1-8.

Ji, M., Hu, Z., Hou, C., Liu, H., Ngo, H. H., Guo, W., . . . Zhang, J. (2020). New insights for enhancing the performance of constructed wetlands at low temperatures. *Bioresource Technology, 122722*.

JICA. (March 2003). *Manual on flood control planning.* Department of public works and highways.

Jim, C. Y., & Chen, W. Y. (2008). Assessing the ecosystem service of air pollutant removal by urban trees in Guangzhou (China). *Journal of environmental management, 88(4)*, pp. 665-676.

Kadlec, R. H., & Reddy, K. R. (2001). Temperature effects in treatment wetlands. *Water environment research, 73(5)*, pp. 543-557.

Kakaras, E., Doukelis, A., Prelipceanu, A., & Karellas, S. (2006). Inlet air cooling methods for gas turbine based power plants.

Kaldellis, J., & Fragos, P. (2011). Ash deposition impact on the energy performance of photovoltaic generators. *Journal of cleaner production, 19(4)*, pp. 311-317.

Kappos, L., Ntouros, I., & Palivos, I. (1996). Pollution effect on PV system efficiency. *Proceedings of the 5th National Conference on Soft Energy Forms.* Athens.

Kivi, R. (2017, Avril 24). *How Does Geothermal Energy Work?* Récupéré sur Sciencing: https://sciencing.com/geothermal-energy-work-4564716.html

Kloss, C., & Calarusse, C. (2011). *Rooftops to Rivers: Green strategies for controlling stormwater and combined sewer overflows.* New-York.

Koc, C. B., Osmond, P., & Peters, A. (2018). Evaluating the cooling effects of green infrastructure: A systematic review of methods, indicators and data sources. *Solar Energy, 166*, pp. 486-508.

Koch, H., & Vögele, S. (2009). Dynamic modelling of water demand, water availability and adaptation strategies for power plants to global change. *Ecological Economics, 68(7)*, pp. 2031-2039.

Kosa, P. (2011). The effect of temperature on actual evapotranspiration based on Landsat 5 TM Satellite Imagery. *Evapotranspiration, 56(56)*, pp. 209-228.

Krishna, P., Kumar, K., & Bhandari, N. M. (2002). IS: 875 (Part3): Wind loads on buildings and structures-proposed draft & commentary. Document No.: IITK-GSDMA-Wind, 02-V5. Roorkee, Uttarakhand, India: Department of Civil Engineering; Indian Institute of Technology Roorkee.

Kumpulainen, L., Laaksonen, H., Komulainen, R., Martikainen, A., Lehtonen, M., Heine, P., . . . Saaristo, H. (2007 ). *Distribution Network 2030 - Vision of the future power system.* Finland: VTT.

Land, M., Granéli, W., Grimvall, A., Hoffmann, C. C., Mitsch, W. J., Tonderski, K. S., & Verhoeven, J. T. (2016). How effective are created or restored freshwater wetlands for nitrogen and phosphorus removal? A systematic review. *Environmental Evidence, 5*.

Larsen, P., Goldsmith, S., Wilson, M., Strzepek, K., Chinowsky, P., & Saylor, B. (2008). Estimating future costs for Alaska public infrastructure at risk from climate. *Global Environmental Change*, pp. 442-457.

Lavin, P. (2003). *A Practical Guide to Design, Production, and Maintenance for Architects and Engineers.* London/New-York: Spon Press.

Law, Y., Ye, L., Pan, Y., & Yuan, Z. (2012). Nitrous oxide emissions from wastewater treatment processes. *Philosophical Transactions of the Royal Society B: Biological Sciences, 367(1593)*, pp. 1265-1277.

Linnerud, K., Mideksa, T. K., & Eskeland, G. S. (2011). The impact of climate change on nuclear power supply. *The Energy Journal, 32(1)*.

Lise, W., & van der Laan, J. (2015). Investment needs for climate change adaptation measures of electricity power plants in the EU. *Energy for Sustainable Development, 28*, pp. 10-20.

Mamo, G. E., Marence, M., Hurtado, J. C., & Franca, M. J. (2018). Optimization of Run-of-River Hydropower Plant Capacity.

Manoli, G., Fatichi, S., Schläpfer, M., Yu, K., Crowther, T. W., Meili, N., . . . Bou-Zeid, E. (2019). Magnitude of urban heat islands largely explained by climate and population. *Manoli, G., Fatichi, S., Schläpfer, M., Yu, K., Crowther, T. W., Meili, N., ... & Bou-Zeid, E. (2019). Magnitude of urban Nature, 573(7772)*, pp. 55-60.

Manwell, J. F., McGowan, J. G., & Rogers, A. L. (2010). *Wind energy explained: theory, design and application.* John Wiley & Sons.

Manwell, J., McGowan, J., & Rogers, A. (2002). *Wind Energy Explained: Theory, Design and Application.*

Maulbetsch, J. S., & Di Filippo, M. N. (2006). *Cost and value of water use at combined-cycle power plants.* California: California Energy Commission - Public Interest Energy Research Program.

Maupoux, M. (2010). *Solar photovoltaic water pumping.* Récupéré sur Practical Action - The Schumacher Centre for Technology and Development :

https://sswm.info/sites/default/files/reference_attachments/MAUPOUX%202010%20Solar%20Water%20Pumping.pdf

Meral, M. E., & Dincer, F. (2011). A review of the factors affecting operation and efficiency of photovoltaic based electricity generation systems. *Renewable and Sustainable Energy Reviews, 15(5)*, pp. 2176-2184.

Mimikou, M. A., & Baltas, E. A. (1997). Climate change impacts on the reliability of hydroelectric energy production. *Hydrological Sciences Journal, 42(5)*, pp. 661-678.

Miradi, M. (2004). Artificial neural network (ANN) models for prediction and analysis of ravelling severity and material composition properties. *CIMCA*, pp. 892-903.

Mirgol, B., Nazari, M., & Eteghadipour, M. (2020). Modelling Climate Change Impact on Irrigation Water Requirement and Yield of Winter Wheat (Triticum aestivum L.), Barley (Hordeum vulgare L.), and Fodder Maize (Zea mays L.) in the Semi-Arid Qazvin Plateau, Iran. *Agriculture, 10(3), 60*.

Mourshed, M. (2012). Relationship between annual mean temperature and degree-days. *Energy and buildings, 54*, pp. 418-425.

N.D. Lea International. (1995). *Modelling Road Deterioration and Maintenance.* Prepared for the Asian Development Bank.

N.D. Lea International. (1995). *Modelling Road Deterioration and Maintenance.* Prepared for the Asian Development Bank.

National Snow & Ice Data Center. (n.d.). *freezing degree-days*. Retrieved from https://nsidc.org/cryosphere/glossary/term/freezing-degree-days

Nazahiyah, R., Yusop, Z., & Abustan, I. (2007). Stormwater quality and pollution loading from an urban residential catchment in Johor, Malaysia. *Water science and technology, 56(7)*, pp. 1-9.

Nemry, F., & Demirel, H. (2012). *Impacts of Climate Change on Transport: A focus on road and rail transport infrastructures.* Luxembourg: Publications Office of the European Union.

Nichol, J. E. (1996). High-resolution surface temperature patterns related to urban morphology in a tropical city: A satellite-based study. *Journal of applied meteorology, 35(1)*, pp. 135-146.

Nordhaus, W. (2017). Revisiting the social cost of carbon. *PNAS*, vol. 11, no.7, 1518-1523.

Nowak, D. J., Greenfield, E. J., Hoehn, R. E., & Lapoint, E. (2013). Carbon storage and sequestration by trees in urban and community areas of the United States. *Environmental pollution, 178, 229-236.*, pp. 229-236.

Ould-Amrouche, S., Rekioua, D., & Hamidat, A. (2010 ). Modelling photovoltaic water pumping systems and evaluation of their CO2 emissions mitigation potential. *Applied Energy, 87*, pp. 3451-3459.

Panagea, I. S., Tsanis, I. K., Koutroulis, A. G., & Grillakis, M. G. (2014). Climate change impact on photovoltaic energy output: the case of Greece. *Advances in Meteorology*.

Pande, P., & Telang, S. (2014). Calculation of Rainwater Harvesting Potential by Using Mean Annual Rainfall, Surface Runoff and Catchment Area. *Green Clean Guide, India, Global Advanced Research Journal of Agricultural Science, Vol 3(7)*, 200-204.

Parker, J. H. (1989, February). The impact of vegetation on air conditioning consumption. *In Proceedings of the Workshop on Saving Energy and Reducing Atmospheric Pollution by Controlling Summer Heat Islands (pp. 45-52).*

Parliamentary Office of Science and Technology (POST). (2011). *Carbon footprint of electricity generation.* Récupéré sur POST Note Update, 383: https://www.parliament.uk/documents/post/postpn_383-carbon-footprint-electricity-generation.pdf

Pérez, G., Coma, J., Martorell, I., & Cabeza, L. F. (2014). Vertical Greenery Systems (VGS) for energy saving in buildings: A review. *Renewable and Sustainable Energy Reviews, 39*, pp. 139-165.

Petchers, N. (2003). *Combined heating, cooling & power handbook: technologies & applications: an integrated approach to energy resource optimization.* Fairmont Press.

Photovoltaic Softwares. (2020). *Photovoltaic Softwares*. Récupéré sur photovoltaic-software.com: https://photovoltaic-software.com/principle-ressources/how-calculate-solar-energy-power-pv-systems

Pierson Jr, W., & Moskowitz, L. (1964). A proposed spectral form for fully developed wind seas based on the similarity theory of SA Kitaigorodskii. *Journal of geophysical research*, pp. 5181-5190.

Plósz, B. G., Liltved, H., & Ratnaweera, H. (2009). Climate change impacts on activated sludge wastewater treatment: a case study from Norway. *Water Science and Technology, 60(2)*, pp. 533-541.

Poullain, J. (2012). *PDHonline Course H119 (2 PDH) - Estimating Storm Water Runoff.* Récupéré sur pdhonline.org: https://pdhonline.com/courses/h119/stormwater%20runoff.pdf

Prado, R. T., & Ferreira, F. L. (2005). Measurement of albedo and analysis of its influence the surface temperature of building roof materials. *Energy and Buildings, 37(4)*, 295-300.

Rademaekers, K., van der Laan, J., Boeve, S., Lise, W., van Hienen, J., Metz, B., . . . Kirchsteiger, C. (2011). *Investment needs for future adaptation measures in EU nuclear power plants and other electricity generation technologies due to effects of climate change* . Brussels: Library (DM28, 0/36).

Ramos-Scharron, C., & MacDonald, L. (2007). Runoff and suspended sediment yields from an unpaved road segment. *Hydrological Processes, 21(1)*, pp. 35-50.

Rodell, M., Chen, J., Kato, H., Famiglietti, J. S., Nigro, J., & Wilson, C. R. (2007). Estimating groundwater storage changes in the Mississippi River basin (USA) using GRACE. *Hydrogeology Journal 15[1]*, pp. 159-166.

Roorda, J., & van der Graaf, J. (2000). Understanding membrane fouling in ultrafiltration of WWTP-effluent. *Water Science and Technology 41(10-11)*, pp. 345-353.

Rousseau, Y. (2013). Impact of Climate Change on Thermal Power Plants. Case study of thermal power plants in France.

Sahely, H. R., MacLean, H. L., Monteith, H. D., & Bagley, D. M. (2006). Comparison of on-site and upstream greenhouse gas emissions from Canadian municipal wastewater treatment facilities. *Journal of Environmental Engineering and Science, 5(5)*, pp. 405-415.

Saito, I., Ishihara, O., & Katayama, T. (1990). Study of the effect of green areas on the thermal environment in an urban area. *Energy and buildings, 15(3-4)*, pp. 493-498.

Santamouris, M. (2014). Cooling the cities–a review of reflective and green roof mitigation technologies to fight heat island and improve comfort in urban environments. *Solar energy, 103*, pp. 682-703.

Scheehle, E. A., & Doorn, M. R. (2012). *Estimate of United States GHG Emissions from wastewater.* Récupéré sur EPA.org: https://www3.epa.gov/ttn/chief/conference/ei12/green/present/scheele.pdf

Scheehle, E. A., & Doorn, M. R. (2012). *Improvements to the U.S. Wastewater Methane and Nitrous Oxide Emissions.* Récupéré sur EPA.org: https://www3.epa.gov/ttn/chief/conference/ei12/green/scheehle.pdf

Schnetzer, J., & Pluschke, L. (2017). *Solar-Powered Irrigation Systems: A clean-energy, low-emission option for irrigation development and modernization.* FAO.

Shukla, A. K., & Singh, O. (2014). Effect of Compressor Inlet Temperature & Relative Humidity on Gas Turbine Cycle Performance. *International Journal of Scientific & Engineering Research, 5(5)*, 664-670.

Shukla, A. K., & Singh, O. (2014). Effect of Compressor Inlet Temperature & Relative Humidity on Gas Turbine Cycle Performance. *International Journal of Scientific & Engineering Research, 5(5)*, 664-670.

Singh, S., & Kumar, R. (2012). Ambient air temperature effect on power plant performance. *International Journal of Engineering Science and Technology*.

Singh, S., & Tiwari, S. (2019). *Climate Change, Water and Wastewater Treatment: Interrelationship and Consequences.* Singapore: Springer.

Song, Z., Zheng, Z., Li, J., Sun, X., Han, X., Wang, W., & Xu, M. (2006). Seasonal and annual performance of a full-scale constructed wetland system for sewage treatment in China. *Ecological Engineering, 26(3)*, pp. 272-282.

Souch, C. A., & Souch, C. (1993). The effect of trees on summertime below canopy urban climates: a case study Bloomington. *Journal of Arboriculture, 19(5)*, pp. 303-312.

Taha, H. (1996). Modeling impacts of increased urban vegetation on ozone air quality in the South Coast Air Basin. *Atmospheric Environment, 30(20)*, pp. 3423-3430.

Taha, H. (1997). Urban climates and heat islands; albedo, evapotranspiration, and anthropogenic heat. *Energy and buildings, 25(2).*

Taha, H., Akbari, H., & Rosenfeld, A. (1988). Vegetation Canopy Micro-Climate: A Field-Project in Davis, California. *Journal of Climate and Applied Meteorology*.

Taha, H., Akbari, H., & Rosenfeld, A. (1991). Heat island and oasis effects of vegetative canopies: micro-meteorological field-measurements. *Theoretical and Applied Climatology, 44(2)*, pp. 123-138.

Tallis, M., Taylor, G., Sinnett, D., & Freer-Smith, P. (2011). Estimating the removal of atmospheric particulate pollution by the urban tree canopy of London, under current and future environments. *Landscape and Urban Planning, 103(2)*, pp. 129-138.

Tang, H. (2012). Research on Temperature and Salt Migration Law of Sulphate Salty Soil Subgrade in Xinjiang Region. Beijing, China: Beijing Jiaotong University.

Taylor, C. R., Hook, P. B., Stein, O. R., & Zabinski, C. A. (2011). Seasonal effects of 19 plant species on COD removal in subsurface treatment wetland microcosms. *Ecological Engineering, 37(5)*, pp. 703-710.

Tiwary, A., Sinnett, D., Peachey, C., Chalabi, Z., Vardoulakis, S., Fletcher, T., . . . Hutchings, T. R. (2009). An integrated tool to assess the role of new planting in PM10 capture and the human health benefits: A case study in London. *Environmental pollution, 157(10)*, pp. 2645-2653.

Tran, Q. K., Jassby, D., & Schwabe, K. A. (2017). The implications of drought and water conservation on the reuse of municipal wastewater: Recognizing impacts and identifying mitigation possibilities. *Water research, 124*, 472-481.
Tsihrintzis, V. A., & Hamid, R. (1998). Runoff quality prediction from small urban catchments using SWMM. *Hydrological Processes, 12(2)*, pp. 311-329.
U.S. DoE. (2013). *U.S. Energy sector vulnerabilities to climate change and extreme weather.* DOE/PI-0013: U.S. Department of Energy.
U.S. Environmental Protection Agency. (2003, September). *Cooling summertime temperatures: Strategies to reduce heat islands.* Récupéré sur epa.gov: https://www.epa.gov/sites/production/files/2014-06/documents/hiribrochure.pdf
Ullrich, A., & Volk, M. (2009). Application of the Soil and Water Assessment Tool (SWAT) to predict the impact of alternative management practices on water quality and quantity. *Agricultural Water Management, 96(8)*, pp. 1207-1217.
UNEP. (2015). *Economic Valuation of Wastewater - The Cost of Action and the Cost of No Action.* United Nations Environment Programme (UNEP), commissioned by the Global Programme of Action for the Protection of the Marine Environment from Land-based Activities (GPA), through the Global Wastewater Initiative (GW2I).
URS Corporation Limited. (2010). *Adapting Energy, Transport and Water Infrastructure to the Long-term Impacts of Climate Change* . San Francisco, CA, USA, Report RMP/5456.
Valkama, P., Mäkinen, E., Ojala, A., Vahtera, H., Lahti, K., Rantakokko, K., . . . Wahlroos, O. (2017). Seasonal variation in nutrient removal efficiency of a boreal wetland detected by high-frequency on-line monitoring. *Ecological engineering, 98*, pp. 307-317.
Van Vliet, M. T., Yearsley, J. R., Ludwig, F., Vögele, S., Lettenmaier, D. P., & Kabat, P. (2012). Vulnerability of US and European electricity supply to climate change. *Nature Climate Change, 2(9)*, 676-681.
Vought, T. D. (2019, June 30). *An Economic Case for Facility Lightning Protection Systems in 2017*. Récupéré sur VFC: https://vfclp.com/articles/an-economic-case-for-facility-lightning-protection-systems-in-2017/
Watkins, R., Littlefair, P., Kolokotroni, M., & Palmer, J. (2002). The London heat island–Surface and air temperature measurements in a park and street gorges. *ASHRAE Transactions, 108(1)*, pp. 419-427.
Wilbanks, T., Bhatt, V., Bilello, D., Bull, S., Ekmann, J., Horak, W., & Huang, Y. J. (2008). *Effects of Climate Change on Energy Production and Use in the United States.* Lincoln: US Department of Energy Publications.
Xiao, Q., & McPherson, E. G. (2002). Rainfall interception by Santa Monica's municipal urban forest. *Urban ecosystems, 6(4)*, pp. 291-302.
Yamba, F., Walimwipi, H., Jain, S., Zhou, P., Cuamba, B., & Mzezewa, C. (2011). Climate change/variability implications on hydroelectricity generation in the Zambezi River Basin. *Mitigation and Adaptation Strategies for Global Change*, pp. 617-628.
Young, I. R., & Holland, G. J. (1996). Atlas of the oceans: wind and wave climate. *Oceanographic Literature Review, 7(43), 742*.
Yuan, H., Nie, J., Zhu, N., Miao, C., & Lu, N. (2013). Effect of temperature on the wastewater treatment of a novel anti-clogging soil infiltration system. *Ecological engineering, 57*, pp. 375-379.

Zhang, C., Liao, H., & Mi, Z. (2019). Climate impacts: temperature and electricity consumption. *Natural Hazards, 99(3)*, pp. 1259-1275.
Zhang, Y., Kendy, E., Qiang, Y., Changming, L., Yanjun, S., & Hongyong, S. (2004). Effect of soil water deficit on evapotranspiration, crop yield, and water use efficiency in the North China Plain. *Agricultural Water Management, 64*(2), pp. 107-122.
Zhao, C., Liu, B., Piao, S., Wang, X., Lobell, D., Huang, Y., . . . ... (2017). Temperature increase reduces global yields of major crops in four independent estimates. *Proceedings of the National Academy of Sciences, 114 (35)*. doi:https://doi.org/10.1073/pnas.1701762114
Zhao, M., Kong, Z. H., Escobedo, F. J., & Gao, J. (2010). Impacts of urban forests on offsetting carbon emissions from industrial energy use in Hangzhou, China. *Journal of Environmental Management, 91(4)*, pp. 807-813.
Zhao, X., Shen, A., & Ma, B. (2018). Temperature Adaptability of Asphalt Pavement to High Temperatures and Significant Temperature Differences. *Advances in Materials Science and Engineering*.
Zheng, S., Huang, G., Zhou, X., & Zhu, X. (2020). Climate-change impacts on electricity demands at a metropolitan scale: A case study of Guangzhou, China. *Applied Energy, 261, 114295*.
Zhou, Z. C., Shangguan, Z. P., & Zhao, D. (2006). Modeling vegetation coverage and soil erosion in the Loess Plateau Area of China. *Ecological modelling, 198(1-2)*, pp. 263-268.
Zoppou, C. (2001). Review of urban storm water models. *Environmental Modelling & Software, 16(3)*, pp. 195-231.
Zouboulis, A., & Tolkou, A. (2016). Effect of climate change in wastewater treatment plants: reviewing the problems and solutions. Dans S. A. Shrestha, *Managing Water Resources under Climate Uncertainty* (pp. 197-220). Springer.
Zoulia, I., Santamouris, M., & Dimoudi, A. (2009). Monitoring the effect of urban green areas on the heat island in Athens. *Environmental monitoring and assessment, 156(1-4)*.
Zsirai, T., Buzatu, P., Maffettone, R., & Judd, S. (2012, April). *Sludge viscosity—The thick of it*. Récupéré sur The MBR (Membrane Bioreactors): https://www.thembrsite.com/features/sludge-viscosity-in-membrane-bioreactors-the-thick-of-it/

# Annex I: Code for establishing the CDS Toolbox-SAVi link

Code related to offline processing of CDS Toolbox and CDS API data for the C3S_428h_IISD-EU project.

### How does this code relate to the CDS API ?

This code builds on the powerful CDS API but focuses on local impact analysis specific for the C3S_428h_IISD-EU project. It makes it easier to retrieve a time series for a specific location or region, and save the result to a CSV file (a simpler format than netCDF for most climate adaptation practitioners). Additionally, the code combines variables across multiple datasets, aggregate them into asset classes (such as all energy-related variables) and perform actions such as bias correction (use of ERA5 and CMIP5).

### Code available for download

The easy way is to download the zipped archive: - latest (development): https://github.com/perrette/iisd-cdstoolbox/archive/master.zip - or check stable releases with description of changes: https://github.com/perrette/iisd-cdstoolbox/releases (see assets at the bottom of each release to download a zip version)

The hacky way is to use git (only useful during development, for frequent updates, to avoid having to download and extract the archive every time):

- First time: `git clone https://github.com/perrette/iisd-cdstoolbox.git`

- Subsequent updates: `git pull` from inside the repository

### Installation steps

- Download the code (see above) and inside the folder.
- Install Python 3, ideally Anaconda Python which comes with pre-installed packages
- Install the CDS API key: https://cds.climate.copernicus.eu/api-how-to
- Install the CDS API client: pip install cdsapi
- Install other dependencies: conda install --file requirements.txt or pip install -r requirements.txt
- *Optional* dependency for coastlines on plots: conda install -c conda-forge cartopy or see docs
- *Optional* dependency: CDO (might be needed later, experimental): conda install -c conda-forge python-cdo

Troubleshooting: - If install fails, you may need to go through the dependencies in requirements.txt one by one and try either pip install or conda install or other methods specific to that dependency. - In the examples that follow, if you have both python2 and python3 installed, you might need to replace python with python3.

## CDS API

Download indicators associated with one asset class.

**Examples of use**:

```
python download.py --asset energy --location Welkenraedt
```

The corresponding csv time series will be stored in `indicators/welkenraedt/energy`. Note that raw downloaded data from the CDS API (regional tiles in netcdf format, and csv for the required lon/lat, without any correction) are stored under `download/` and can be re-used across multiple indicators.

The `indicators` folder is organized by location, asset class, simulation set and indicator name. The aim is to provide multiple sets for SAVi simulation. For instance, `era5` for past simulations, and various `cmip5` versions for future simulations, that may vary with model and experiment. For instance the above command creates the folder structure (here a subset of all variables is shown):

```
indicators/
  welkenraedt/
    energy/
      era5/
        2m_temperature.csv
        precipitation.csv
        ...
      cmip5-ipsl_cm5a_mr-rcp_8_5/
        2m_temperature.csv
        precipitation.csv
        ...
      ...
```

with two simulation sets `era5` and `cmip5-ipsl_cm5a_mr-rcp_8_5`. It is possible to specify other models and experiment via `--model` and `--experiment` parameters, to add further simulation sets and thus test how the choice of climate models and experiment affect the result of SAVi simulations.

Compared to raw CDS API, some variables are renamed and scaled so that units match and are the same across simulation sets. For instance, temperature was adjusted from Kelvin to degree Celsius, and precipitation was renamed and units-adjusted into mm per month from original (mean_total_precipitation_rate (mm/s) in ERA5, and mean_precipitation_flux (mm/s) in CMIP5). Additionally, CMIP5 data is corrected so that climatological mean matches with ERA5 data (climatology computed over 1979-2019 by default).

Additionally to the files shown in the example folder listing above, figures can also be created for rapid control of the data, either for interactive viewing (`--view-timeseries` and `--view-region`) or or saved as PNG files (`--png-timeseries` and `--png-region`), e.g.

```
python download.py --asset energy --location Welkenraedt --png-timeseries --
png-region
```

Single indicators can be downloaded via:

```
python download.py --indicator 2m_temperature --location Welkenraedt
```

The choices available for `--indicator` , `--asset` and `--location` area defined in the following configuration files, respectively:

- controls which indicators are available, how they are renamed and unit-adjusted: indicators.yml (see sub-section below)
- controls the indicator list in each asset class: assets.yml
- controls the list of locations available: locations.yml

Full documentation, including fine-grained controls, is provided in the command-line help:

```
python download.py --help
```

Visit the CDS Datasets download pages, for more information about available variables, models and scenarios:

- ERA5: https://cds.climate.copernicus.eu/cdsapp#!/dataset/reanalysis-era5-single-levels-monthly-means?tab=form

- CMIP5: `https://cds.climate.copernicus.eu/cdsapp#!/dataset/projections-cmip5-monthly-single-levels?tab=form`

In particular, clicking on "Show API request" provides information about spelling of the parameters, e.g. that "2m temperature" is spelled `2m_temperature` and "RCP 8.5" is spelled `rcp_8_5`.

### Indicator definition

This section is intended for users who wish to extend the list of indicators currently defined in indicators.yml. It can be safely ignored for users who are only interested in using the existing indicators.

Let's see how `10m_wind_speed` is defined:

```
- name: 10m_wind_speed
  units: m / s
  description: Wind speed magnitude at 10 m
```

The fields `name` and `units` define the indicator. Description is optional, just to provide some context. It is possible to provide `scale` and `offset` fields to correct the data as `(data + offset) * scale`. Here for `2m temperature`:

```
- name: 2m_temperature
  units: degrees Celsius
  description: 2-m air temperature
  offset: -273.15  # Kelvin to degrees C
```

# denotes a comment to provide some context. Some indicators have different names in ERA5 and CMIP5, and possibly different units. That can be dealt with by providing `era5` and `cmip5` fields, which have precedence over the top-level fields. Here the `evaporation` definition:

```
- name: evaporation
  units: mm per month
  era5:
    name: mean_evaporation_rate  # different name in ERA5
    scale: -2592000  # change sign and convert from mm/s to mm / month
  cmip5:
    scale: 2592000  # mm/s to mm / month
```

In that case both scaling and name depend on the dataset. In CMIP5 which variable name is identical to our indicator name, the `name` field can be omitted. In ERA5, evaporation is negative (downwards fluxes are counted positively), whereas it is counted positively in ERA5.

Indicators composed of several CDS variables can be defined via `compose` and `expression` fields. Let's look at `100m_wind_speed`:

```
- name: 100m_wind_speed
  units: m / s
  description: Wind speed magnitude at 100 m
  era5:
    compose:
      - 100m_u_component_of_wind
      - 100m_v_component_of_wind
    expression: (_100m_u_component_of_wind**2 + _100m_v_component_of_wind**2)
**0.5
  cmip5:
    name: 10m_wind_speed
    scale: 1.6  # average scaling from 10m to 100m, based on one test locatio
n (approximate!)
```

In ERA5, vector components of 100m wind speed are provided. Our indicator is therefore a composition of these two variables, defined by the `expression` field, which is evaluated as a python expression. Note that variables that start with a digit are not licit in python and must be prefixed with an underscore _ in the `expression` field (only there).

For complex expressions, it is possible to provide a `mapping` field to store intermediate variables, for readability. This is used for the `relative_humidity` indicator:

```
- name: relative_humidity
  units: '%'
  era5:
    compose:
```

```
      - 2m_temperature
      - 2m_dewpoint_temperature
    expression: 100*(exp((17.625*TD)/(243.04+TD))/exp((17.625*T)/(243.04+T)))
    mapping: {T: _2m_temperature - 273.15, TD: _2m_dewpoint_temperature - 273
.15}
  cmip5:
    name: near_surface_relative_humidity
```

where `T` and `TD` are provided as intermediary variables, to be used in `expression`.

ERA5-hourly dataset can be retrieved via `frequency: hourly` field, and subsequently aggregated to monthly indicators thanks to pre-defined functions `daily_max`, `daily_min`, `daily_mean`, `monthly_mean`, `yearly_mean`. For instance:

```
- name: maximum_daily_temperature
  units: degrees Celsius
  offset: -273.15
  cmip5:
    name: maximum_2m_temperature_in_the_last_24_hours
  era5:
    name: 2m_temperature
    frequency: hourly
    transform:
      - daily_max
      - monthly_mean
```

This variable is available directly for CMIP5, but not in ERA5. It is calculated from `2m_temperature` from ERA5 hourly dataset, and subsequently aggregated. Note the ERA5-hourly dataset takes significantly longer to retrieve than ERA5 monthly. Consider using in combination with `--year 2000` to retrieve a single year of the ERA5 dataset.

Currently CMIP5 daily is not supported.

### Netcdf to csv conversion

Convert netcdf time series files downloaded from the CDS Toolbox pages into csv files (note: this does not work for netcdf files downloaded via the cds api):

```
python netcdf_to_csv.py data/*nc
```

Help:

```
python netcdf_to_csv.py --help
```

Copernicus Climate Change Service